Biomaterials 115 (2017) 40–52

Contents lists available at ScienceDirect

Biomaterials

journal homepage: www.elsevier.com/locate/biomaterials

A biomaterial-assisted mesenchymal stromal cell therapy alleviates colonic radiation-induced damage

Lara Moussa [a, b, c], Girish Pattappa [b, c], Bastien Doix [a], Sarra-Louiza Benselama [a], Christelle Demarquay [a], Marc Benderitter [a], Alexandra Sémont [a], Radia Tamarat [a], Jérôme Guicheux [b, c, d], Pierre Weiss [b, c, d], Gildas Réthoré [b, c, d], Noëlle Mathieu [a, *]

[a] IRSN, Institut de Radioprotection et de Sûreté Nucléaire, Laboratoire de Recherche en Régénération des tissus sains Irradiés (LR2I), 31 Avenue de la Division Leclerc, 92262 Fontenay-aux-Roses, France
[b] INSERM, Institut National de la Santé et de la Recherche Médicale, UMRS 791, Laboratoire d'Ingénierie Ostéo-Articulaire et Dentaire (LIOAD), Faculté de Chirurgie Dentaire, 1 Place Alexis Ricordeau, 44042 Nantes, France
[c] Université de Nantes, Laboratoire d'Ingénierie Ostéo-Articulaire et Dentaire (LIOAD), Faculté de Chirurgie Dentaire, 1 Place Alexis Ricordeau, 44042 Nantes, France
[d] Centre Hospitalier Universitaire de Nantes, Pôle Hospitalo-Universitaire 4 (OTONN), 1 Place Alexis Ricordeau, 44042 Nantes, France

ARTICLE INFO

Article history:
Received 28 September 2016
Received in revised form
14 November 2016
Accepted 14 November 2016
Available online 16 November 2016

Keywords:
Colorectal irradiation
Mesenchymal stromal cells
Hydrogel
Colonic permeability
Regenerative medicine
Injection through colonoscopy

ABSTRACT

Healthy tissues surrounding abdomino-pelvic tumours can be impaired by radiotherapy, leading to chronic gastrointestinal complications with substantial mortality. Adipose-derived Mesenchymal Stromal Cells (Ad-MSCs) represent a promising strategy to reduce intestinal lesions. However, systemic administration of Ad-MSCs results in low cell engraftment within the injured tissue. Biomaterials, able to encapsulate and withstand Ad-MSCs, can overcome these limitations. A silanized hydroxypropylmethyl cellulose (Si-HPMC) hydrogel has been designed and characterized for injectable cell delivery using the operative catheter of a colonoscope. We demonstrated that hydrogel loaded-Ad-MSCs were viable, able to secrete trophic factors and responsive to the inflammatory environment. In a rat model of radiation-induced severe colonic damage, Ad-MSC + Si-HPMC improve colonic epithelial structure and hyperpermeability compared with Ad-MSCs injected intravenously or locally. This therapeutic benefit is associated with greater engraftment of Si-HPMC-embedded Ad-MSCs in the irradiated colonic mucosa. Moreover, macrophage infiltration near the injection site was less pronounced when Ad-MSCs were embedded in the hydrogel. Si-HPMC induces modulation of chemoattractant secretion by Ad-MSCs that could contribute to the decrease in macrophage infiltrate. Si-HPMC is suitable for cell delivery by colonoscopy and induces protection of Ad-MSCs in the tissue potentiating their therapeutic effect and could be proposed to patients suffering from colon diseases.

1. Introduction

Radiotherapy plays a crucial in the management of malignant pelvic diseases. However, the major limitation of this treatment is its toxicity on surrounding healthy tissues such as the small intestine, colon and rectum. Due to the high proliferative capacity of epithelial stem cells located at the base of the crypts, the gut is a very radiosensitive organ. Irradiation produces free radicals that, through direct and indirect effects, induce crypt cell apoptosis leading to mucosal lesions with a loss of epithelial barrier function. The intestinal epithelial barrier is maintained by intracellular junctional complexes, such as tight junctions (TJs), adherent junctions and desmosomes. Irradiation increases mucosal permeability, inducing nutrient and fluid loss as well as gut pathogen infiltration, exacerbating mucosal inflammation [1]. This inflammatory state, combined with the deficiency of epithelial stem cells and local ischemia, leads to a defective healing process which can result in tissue loss (ulceration) or pathological healing (fibrosis, fistula) [2].

Patients (10–20%) undergoing radiotherapy for abdominal cancers develop intestinal complications several years after the end

Abbreviations: Ad-MSCs, Adipose-derived Mesenchymal Stromal Cells; Si-HPMC, Silanized HydroxyPropylMethyl Cellulose.

* Corresponding author. IRSN, PRP-HOM/SRBE/LR2I, 92262 Fontenay aux Roses, France.
E-mail address: noelle.mathieu@irsn.fr (N. Mathieu).

http://dx.doi.org/10.1016/j.biomaterials.2016.11.017

of their treatment. These chronic complications adversely affect quality of life and, in some cases, can be life-threatening. Management of patients suffering from radiotherapy-related gastrointestinal disorders is limited to symptomatic treatments. No curative treatments are currently available. Therefore, symptoms reoccur once treatment is stopped and new features may arise depending upon the course of the disease. The lack of curative treatment and the potential severity of the gastrointestinal disorders highlight the importance of finding a novel and effective treatment. Stem cell-based regenerative medicine using mesenchymal stromal cells (MSCs) is considered a promising approach, as suggested by encouraging results from various clinical trials [1].

Convincing experimental results from different animal models [3–5] and in clinical cases treated on a compassionate basis [6,7] have shown that intravenous (IV) injection of MSCs reduces severe colorectal lesions caused by ionizing irradiation. Experiments performed on animal models have shown that IV-MSC treatment promotes epithelial regeneration leading to intestinal structure improvement and limiting the fibrosis process [3–5]. The beneficial effects of MSC injection have been primarily related to their secretion of a wide variety of bioactive molecules [8]. MSCs secrete angiogenic, pro-regenerative, anti-apoptotic and immunosuppressive factors that may contribute to intestinal ulcer wound healing. Moreover, pre-clinical data on mini-pigs has demonstrated that repeated intravenous MSC injections are necessary to improve radio-induced colorectal ulcer healing [9]. These data suggest that MSC-induced therapeutic benefit requires a large number of injected cells. Despite a large amount of MSCs being systemically injected, very low cell engraftment in the irradiated intestine has been reported [3,4]. Indeed, studies have demonstrated that systemically injected MSCs were trapped in the lung after infusion [10]. Although a study from Prockop group has demonstrated that the anti-inflammatory effects of MSCs depend upon their trapping in the lung [11], some studies have demonstrated a pulmonary embolus following intravenous injection of MSCs [12–14]. It is known that MSCs are short-lived when infused intravenously. Indeed, they die within 24 h and are cleared from the body [15]. Thus, local injection of cells has been tested according to the accessibility of the tissue [16]. This injection method allows fewer cells to be injected, increases the rate of MSC engraftment in the area requiring repair and interestingly, for clinical application, reduces the cost of the treatment. Moreover, local injection reduces the spread of stem cells throughout the body, although no side effects have been shown after either local or intravenous injection of MSCs [17,18]. While local injection leads to better cell engraftment, cell viability could be limited due to the host microenvironment, particularly in the case of radiotherapy. After colorectal irradiation, the secretion of pro-inflammatory cytokines as IL1b, TGFb and chemoattractant has been demonstrated, as well as the huge infiltrate of innate immune cells [19,20]. In order to overcome these drawbacks, the use of a hydrogel that entraps the MSCs may protect the cells from the host tissue environment. The cytoprotective properties of the hydrogel could maintain the viability and function of the cells. This biomaterial-assisted cell therapy may make it possible to significantly increase the therapeutic benefit with a reduced number of injections. Indeed, in cases of ischemia (heart and hindlimb), studies have demonstrated that injection of MSCs embedded in biomaterials enhances their therapeutic benefit [21,22]. This method of injection is also used for articular cartilage repair by direct implantation with minimally invasive surgery [23].

Amongst the wide variety of biomaterials, biocompatible hydrogels may represent an excellent cell delivery system in view of their distinctive property of permitting *in-situ* gelation. Two types of hydrogels exist: natural and synthetic. Natural hydrogels are used as scaffolds because they display numerous biological functions that synthetic polymers lack, such as cell adhesion and biodegradation. A hybrid semi-synthetic, semi-biological silanized hydroxypropylmethyl cellulose (Si-HPMC) hydrogel has been designed as an injectable cell carrier. This Si-HPMC hydrogel is biocompatible, able to self-crosslink *in situ* to form a scaffold and maintain MSC phenotype, viability and secretion ability [23]. Indeed, Mathieu et al. have demonstrated the beneficial effect of Si-HPMC hydrogel in cardiac tissue engineering with a pronounced improvement in cardiac capacity after infarction when MSCs were injected within the biomaterial [22].

Here, we aimed to use a Si-HPMC hydrogel with rheological properties compatible with clinical use through a specific colonoscope catheter. We evaluated the effects of hydrogel-assisted Ad-MSC therapy compared with conventional intravenous injections of MSCs as used in clinical applications on structural and functional damage induced on a rat model of colorectal irradiation [4]. We also followed the engraftment of the Ad-MSCs and their fate in the lesion site. Lastly, we studied the hydrogel's ability to protect the cells from the deleterious irradiated environment.

2. Materials and methods

2.1. Ethics statement

All experiments were performed in compliance with the Guide for the Care and Use of Laboratory Animals as published by the French regulations for animal experiments (Ministry of Agriculture Order No. B92-032-01, 2006) with European Directives (86/609/CEE) and were approved by local ethical committee of the institute (permit number P13-14).

2.2. Animals and irradiation protocol

Male SD (Sprague Dawley, non-consanguineous) rats (Janvier SA, Le Genest St Isle, France) weighing 250 g were received and housed in a temperature-controlled room (21 ± 1 °C). They were allowed free access to water and fed standard pellets. Rats were anesthetized by isoflurane inhalation and a single 29 Gray (Gy) dose was delivered by a medical accelerator (Alphée) through a 2 × 3 cm window centered on the colorectal region. Alphée is an accelerator-type radiation source (maximal energy is 4 MeV with an average energy of about 1.5 MeV; 30 kA).

2.3. Cell culture and characterization

Adipose-derived MSCs were obtained by digesting the subcutaneous inguinal adipose tissue of seven-week-old GFP-transgenic SD rats as previously described [5]. After 7 days, the monolayer of adherent cells was trypsinized, washed in PBS three times before injection in rats. The phenotype of amplified Ad-MSC was verified by flow cytometry. The percentage of CD90 (clone OX-7; BD Biosciences, Le pont de Claix, France) and CD73 (clone 5F/B9; BD Biosciences) positive cells were analyzed and the absence of hematopoietic cells was verified with CD34 (clone ICO115, Santa Cruz, Dallas, Texas, USA) and CD45 (clone OX-1; BD Biosciences) markers. Isotype identical antibodies served as controls. On average, Ad-MSC expressed CD90 at 95.25% (±2.7), CD73 at 65.42% (±18.9), CD34 at 1.45% (±1.01) and CD45 at 0.575% (±0.2). The potential of adipogenic and osteogenic differentiations was also evaluated.

2.4. Hydrogel preparation

Hydroxypropyl methyl cellulose (Methocel® E4M Premium procured from Colorcon) was silanized by grafting 3-glycidoxypropyltrimethoxysilane GPTMS as previously described

[24]. Si-HPMC powder was dissolved in NaOH solution (0.2 M) then dialyzed to reach a final pH value of 12.7 [25]. Acidic buffer solution used to neutralize the basic Si-HPMC solution was prepared using 0.1 M HCl and HEPES as previously described [25]. Si-HPMC hydrogels were prepared by rapidly mixing the polymer and the buffer at a ratio of 2:1 leading to a pH of 7.4 and then, initiating silanol condensation.

2.5. Injectability of the hydrogel

The injectability was measured using a compression testing device (TAHDplus) with 5 kg load cell utilized for the measurements. Five kg is the maximum force that can be applied by hand. Si-HPMC at either concentrations of 1% and 1.5% were pre-loaded into the catheter. A syringe containing 1 ml 0.1 M NaCl (Sigma-Aldrich, Germany) was attached to the catheter and the injection force was measured.

2.6. Rheological characteristics

2.6.1. Viscosity

Intrinsic viscosity was measured using a steady shear rate ranging from 0.1 to 100 s^{-1} at room temperature. The subsequent flow curves were fitted using the simplified Cross equation for each of the Si-HPMC concentrations measured to calculate the limiting viscosity [26].

2.6.2. Gel point measurements

The gel point was measured on HAAKE RheoStress RS300 rheometer (Thermo Scientific) using cone/plate geometry (1°/60 mm). Liquid hydrogel precursor solutions were injected on the plate immediately after mixing and the measurements started 1–2 min later. Storage (G') modulus was monitored as a function of time under oscillation frequency sweep (from 1 to 22 Hz) at a constant temperature (23 °C). The gel point was determined when $\tan \delta = G''/G'$ became independent from frequency. Each sample was measured in triplicate.

2.6.3. Elastic modulus measurements

Storage (G′) modulus of fully cross-linked hydrogels was measured using a plate geometry (PP20 Ti) under oscillatory mode with a shear stress ranging from 0.1 to 3000 Pa. Initially, 1% and 1.5% (w/v) Si-HPMC was formulated and poured (2 mL) into 12-well plates. Plates were placed either at room temperature or a 37 °C incubator under a humid atmosphere to prevent drying and allowed to set for 14 days. Plate was loaded onto a specially designed plate platform for the rheometery measurement and then a 0.5 N normal force was applied prior to measurement. G′ for Si-HPMC at each concentration was determined from the graphs.

2.7. Ad-MSC viability, morphology and proliferation within the hydrogel

Cells were seeded at 3.33×10^6 cells/ml with each individual gel containing approximately 1×10^6 cells. Cell viability was evaluated using Calcein AM-ethidium homodimer assay (Live and Dead®, Invitrogen, France) and then observed using a confocal microscope. Images were then assessed using commercial software (Velocity, Nikon corporation) to count the number of green (live) and red (dead) cells from each sample. Samples stained yellow (dual stained red and green) upon analysis were counted as dead cells. Cells were cultured for a 21 day period with live/dead assessment conducted on day 1, 7, 14 and 21 during culture. A set of cells was cultured in the presence of actinomycin D (10 μg/ml) to act as a negative control for the study. Proliferation analyses were realized using immunofluorescence. Cells were loaded on the lab-Tek chamber slide system (Nunc) with or without hydrogel during 72 h in culture medium. After PBS 1X washing, the cells were fixed then permeabilized with TritonX-100 0.5% during 15min and incubated overnight with mouse anti PCNA (M0879, DakoCytomation). Staining was revealed using a fluorescent secondary antibody (1/200eme goat anti-mouse Alexa 488, A11017, Invitrogen). After washing, nuclei were stained with DAPI (Vector Labs).

2.8. Experimental protocol

In two series of experiments, 3 weeks after irradiation, rats were injected with either 5.10^6 or 1.10^6 Ad-MSCs intravenously (IV) or 1.10^6 Ad-MSCs locally injected with or without Si-HPMC (at 1 or 1.5% of concentration) using a colonoscope (Pentax, Argenteuil, France) (see video). For IV injection, 5.10^6 or 1.10^6 of Ad-MSCs were diluted in 500 μl of PBS and injected in the tail vein. For local injection, 1.10^6 of Ad-MSCs was mixed with 300 μl of Si-HPMC (1 or 1.5%) and injected locally using the colonoscope (Supplementary Fig. A,D). A single injector use (Olympus, Rungis, France) of 165 cm of length and 2 mm of diameter connected to a needle (23 Gauge) was used. Two injection points were done, upstream and downstream of the lesion (Supplementary Fig. B,C). Animals were then sacrificed one week later. In the first series, distal colons were dissected, washed in Krebs solution and used for colonic epithelial permeability measurements in Ussing chambers. A second series of experiments was performed where samples of colon were collected for claudin 4 expression by Western blot and for histological and immunohistochemistry staining.

Supplementary video related to this article can be found at http://dx.doi.org/10.1016/j.biomaterials.2016.11.017.

2.9. Ussing chambers experiments

Immediately after the sacrifice, distal colons were removed, cut along the mesenteric border, and three colonic strips from each rat were mounted in Ussing chambers (Corning Costar Corporation, Harvard Apparatus, France) having a flux area of 0.1 cm^2. Colonic epithelial permeability to small and large molecules was measured through the mucosal-to-serosal passage of fluoro isothiocyanate (FITC)-Dextran 4 kDa (FD4) and intact Horseradish peroxidase (HRP) 44 kDa (Sigma-Aldrich, Saint Quentin Fallavier, France), respectively, added simultaneously in the mucosal compartment. After 20 min of equilibration, 600 μl of buffer solution on the mucosal side was replaced by 300 μl of FD4 (2.2 mg/ml, Sigma-Aldrich) and 300 μl of HRP (0.4 mg/ml, Sigma-Aldrich). Electrical parameters, including potential difference, short-circuit current (Isc) and total electrical resistance (R), were recorded at regular intervals during the 2-h period of experimentation. Colonic permeability to FD4 was determined by measuring the fluorescence intensity at 485 nm/525 nm using an automatic Infinite M200 microplate reader (Tecan, Lyon, France). Epithelial permeability to intact HRP was determined by an enzymatic assay [27] for specific HRP activity found in the serosal and mucosal compartment using a microplate reader (Tecan). Permeability was calculated as the ratio of flux/concentration, as previously described [28] and expressed in cm/second.

2.10. Tissue protein extraction and claudin 4 expression by western blot

Tissue proteins were extracted with RIPA buffer (Santa Cruz, Dallas, Texas, USA) with protease inhibitor cocktail (Roche Diagnostics, Meylan, France). Clear lysates were prepared by centrifugation at 10000*g* for 10 min, and protein concentrations were

assessed using the QuantiPro BCA assay kit (Sigma-Aldrich).

Equal protein amounts of each extract were separated in 12.5% SDS-polyacrylamide gel and transferred onto 0.45 mm nitrocellulose membranes (Whatman). Membranes were blocked with 5% dry milk in 0.1% tween in PBS (PBST) for 45 min at RT, and then incubated overnight at 4 °C with either mouse anti-claudin 4 antibody (Life Technologies, Saint-Aubin, France; 1/500) or anti-GAPDH antibody used as internal standard. After washing in PBST−milk, membranes were incubated for 1 h at RT with horseradish peroxidase-conjugated secondary antibody (Amersham ECL Kit; 1/5000) and washed. Bands were identified using Luinata Forte substrate (Merc Millipore, Darmstadt, Germany). Relative values of the band density were estimated using ImageJ software (NIH, Bethesda, MD, USA) and claudin 4 expression was assessed relative to GAPDH for each sample analyzed.

2.11. Histological and lesion analyzes

Animals were sacrificed and immediately after, the irradiated area which corresponds to a white, non-vascularized zone was measured (photos were taken with Zeiss binocular (x 0.6)). Then, the colon was collected and fixed in 4% formaldehyde and embedded in paraffin. Paraffin embedded colons were cut on a rotary microtome (Leica Microsystems AG, Wetzlar, Germany) into serial circular sections of 5 μm, spaced 150 μm (all damaged zone) and stained with hematoxylin-eosin-saffron (HES). The severity of colorectal damage induced by irradiation was assessed using an injury score. Determination of the injury score was based on mucosal damages (ulceration, epithelial atypia, and regenerative crypts), edema, colitis cystica profunda, vascular sclerosis and muscular dystrophy. Graduation of the injury was 0 = null; 10 = slight; 20 = moderate and 30 = severe.

2.12. Immunohistochemistry

For immunohistochemistry (IHC), sections were deparaffinized and hydrated. Serial slides were used for GFP, PCNA and CD68 staining. Tissue sections were treated with 0.1% triton X-100 (Sigma-Aldrich) in PBS 1x (Life Technologies) at room temperature (RT) for 10 min. Then endogenous peroxidases were inhibited by incubation with 3% H_2O_2 in methanol at RT for 10 min. For GFP (Green Fluorescent Protein) IHC, after saturation (X0909, DakoCytomation, Courtaboeuf, France), goat anti-GFP diluted to 1/1000 (ab6673, Abcam, Cambridge, UK) was applied for 1 h at 37 °C. Sections were incubated with impress reagent kit anti-goat Ig (MP7405, Vector) for 20 min at RT. For CD68 IHC, enzymatic retrieval solution (Proteinase K, S3020, DakoCytomation) was performed. After saturation, mouse anti rat CD68 (MCA341R, AbDserotec, Oxford, UK) at 1 mg/mL was applied for 1 h at 37 °C. Sections were incubated with Envision kit anti-mouse HRP (K4002, DakoCytomation) for 30 min at RT. For PCNA (Proliferating Cell Nuclear Antigen) immunostaining, tissue sections were placed in an antigen retrieval solution (0.01 M citrate buffer, pH = 6 (DakoCytomation) for 15 min at 350 W) and quenched for endogenous peroxidases as described above. After saturation, mouse anti PCNA (M0879, DakoCytomation) at 525 μg/ml was applied for 1 h at 37 °C. Sections were incubated with Envision kit anti-mouse HRP for 30 min at RT.

Staining was developed with Histogreen substrate (E109, Eurobio, Les Ulis, France). Then, sections were counterstained with nuclear fast red (H3403, VectorLabs, Burlingame, CA, USA), dehydrated and mounted. Isotype control antibodies are used as negative controls.

2.13. Double staining of GFP and TUNEL

In order to identify if Ad-MSC expressing GFP are apoptotic, double staining of GFP and terminal deoxynucleotidyl transferase-mediated dUTP nick end labeling (TUNEL) was performed. Following immunohistochemical staining of GFP, as described above (using donkey anti-goat Alexa as secondary antibody), the TUNEL was performed using the *In Situ* Cell Death Detection Kit (Roche Diagnostics).

2.14. Secretome analysis

Proteins released from Ad-MSCs during culture in 2D and 3D were quantified following 7 days of culture. On day 6, culture media was aspirated and cells washed using PBS. Medium without serum was added to the cells and then incubated for 24 h. Media was then evaluated for secretome products using commercial rat ELISA kits. Data normalization for the secreted factors required DNA quantification using Picrogreen dsDNA quantification kit (Invitrogen).

2.15. Statistical analysis

All data are presented as mean ± SEM. Statistical analyzes were performed using Graph Pad Prism 5.0 (GraphPad, San Diego, CA). Statistical significance was determined using one-way ANOVA followed by Tukey's post-test for multiple groups, or two-way ANOVA followed by Bonferroni's post-test for multiple groups with different variables, or *t*-test when changes were compared between two groups. Statistical significance was set at $p < 0.05$.

3. Results

3.1. Formulation and characterization of Si-HPMC for colonoscopy procedure

Local treatment for colorectal side effects of radiotherapy can be administered using the operative channel of a colonoscope. Our aim was to determine the appropriate Si-HPMC concentration that provides the best compromise between the injectability within the specific catheter system and optimized cell protection. Si-HPMC viscosity was measured using a rheometer under a variable shear stress. Two Si-HPMCs at final concentrations of 1% and 1.5% (w/v) were tested before cross-linking, and measurements showed an increase in viscosity with Si-HPMC concentration (Table 1). The results showed that, in these conditions, the peak force applied was 1.34 kg for 1% Si-HPMC and 3.52 kg for 1.5% Si-HPMC concentrations (Table 1). These results therefore determined that both Si-HPMC concentrations could be injected through the colonoscope

Table 1
Formulation and characterization of Si-HPMC for colonoscopy procedure. Viscosity, injectability, gel-point and elastic modulus of Si-HPMC at 1% and 1.5%. N = 3. [a]p<0.05 vs. 1% Si-HPMC, [b]p < 0.05 vs. RT, RT = Room Temperature.

Si-HPMC concentration (%)	Viscosity (Pas)	Injectability (kg)	Gel point (min)		Elastic modulus (Pa)	
			RT	37 °C	RT	37 °C
1	0.086 ± 0.016	1.34 ± 0.07	56.5 ± 2.6	19.4 ± 1.3[b]	145 ± 40.6	130.2 ± 20.7
1.5	0.309 ± 0.05[a]	3.52 ± 0.1[a]	41.5 ± 5.9	11.9 ± 1.5[b]	426.8 ± 53.4[a]	380.9 ± 58.2[a]

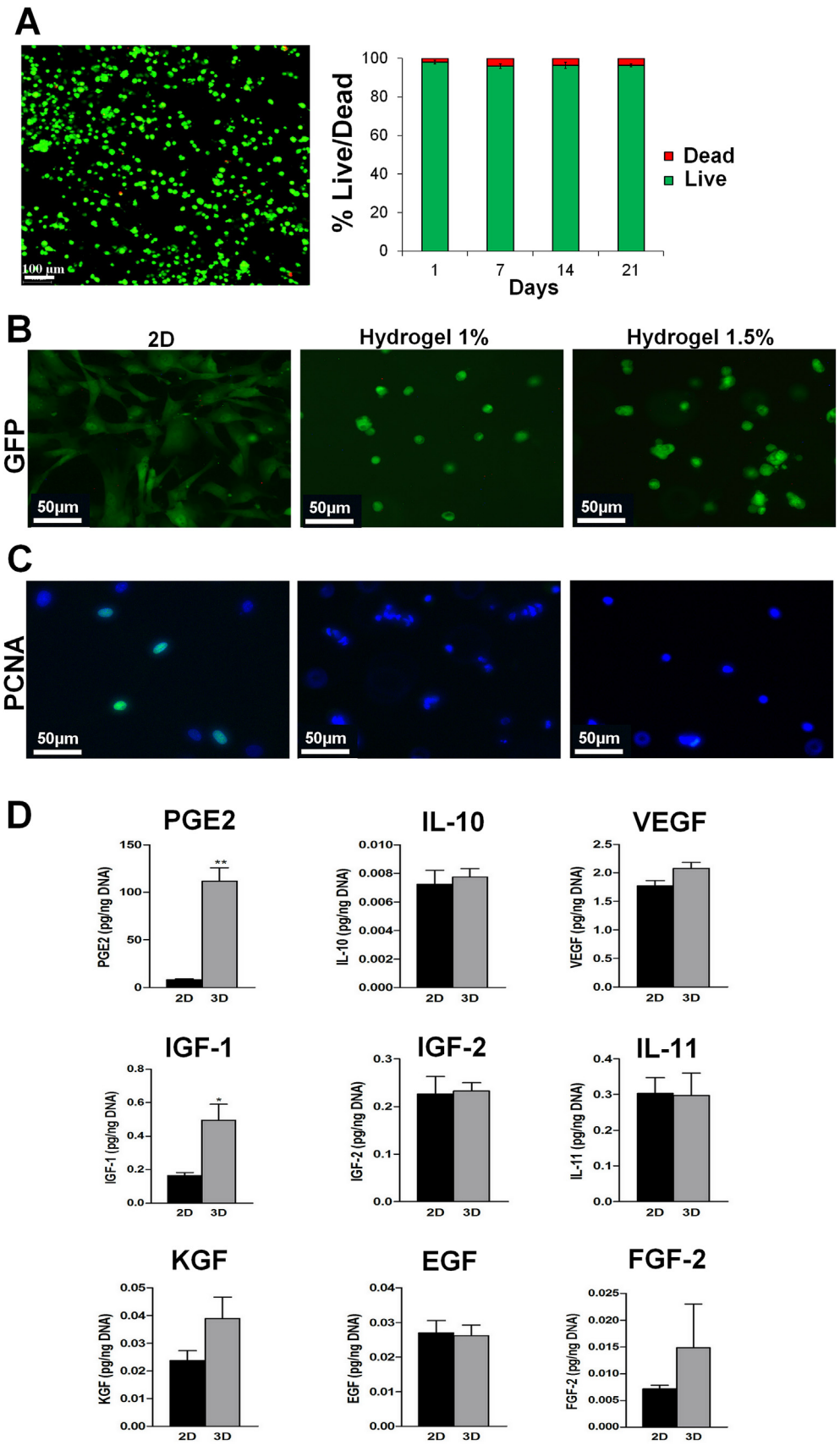

Fig. 1. In vitro cell viability, morphology and secretome analysis within Si-HPMC. (A) Cell viability was evaluated using Live and Dead assay. Live cells are in green and dead ones are in red. Cells stained in yellow (dual stained red and green) upon analysis were counted as dead cells. (B) Morphology of GFP-Ad-MSC in 2D or 1% and 1.5% hydrogel. (C) In vitro proliferation analyses of Ad-MSCs in 2D and in hydrogel with different levels of stiffness. Representative pictures of immunofluorescence staining. Proliferative cells were stained with PCNA marker in green and all the nuclei were stained with dapi in blue. Most of Ad-MSCs were proliferative in 2D (left) and none in 3D whatever the concentration of the hydrogel (middle and right). (D) Secretion factors in supernatants of Ad-MSCs in Si-HPMC compared with two-dimensional Ad-MSCs. Data normalization for the secreted factors required DNA quantification using Picrogreen dsDNA quantification kit. N = 3 donors in triplicate. $^{*}p < 0.05$ vs. 2D, $^{**}p < 0.01$ vs. 2D.

catheter. Table 1 shows that with respect to temperature, the gel-point significantly decreased at body temperature (37 °C) compared to room temperature (21 °C) at both Si-HPMC concentrations ($p < 0.05$). A reduction in the Si-HPMC concentration resulted in an increase in the gel-point, whereby a positive correlation between Si-HPMC concentration and gelation time was found at both temperatures measured ($p < 0.05$). Moreover, a significant difference between Si-HPMC concentrations was found in terms of elastic modulus (G') with a lower value for 1% Si-HPMC compared to 1.5%, when no difference was observed between room and body temperature. However, both values are compatible with soft tissue (i.e. colon) application. Taken together, these analyses determined that 1% and 1.5% Si-HPMC hydrogel have the required properties: Si-HPMC viscosity enables it to be injected at 1% and 1.5% with the colonoscope. Its reticulation kinetic at room temperature is compatible with manipulation by the surgeons in the operating theatre. Moreover, once injected *in vivo* (37 °C), the mechanical properties of the Si-HPMC were not modified and the reticulation time is fast (12–19 min) ensuring optimal cell protection.

3.2. Viability, morphology and secretome analyses of Ad-MSCs embedded in Si-HPMC

The viability of Ad-MSCs in 1% and 1.5% hydrogel has been tested *in vitro* for 21 days. When Ad-MSCs were mixed in 1% Si-HPMC, we observed that not all the cells were entrapped and some cells remained attached to the bottom of the culture plate (data not shown). Cells mixed with a 1.5% Si-HPMC concentration appeared to be fully entrapped within the hydrogel, thus viability and cytokine release were only assessed for this condition. We quantified that 95% of cells were viable after 21 days of culture (Fig. 1A). Morphology of Ad-MSCs embedded in Si-HPMC has been assessed: we observed that cells in 3D have a spherical morphology which is not modified with the stiffness of the hydrogel (Fig. 1B). We observed, in the viability experiments, that the number of cells is not modified with time. To verify the lack of proliferation in the hydrogel, we used PCNA (Proliferating Cell Nuclear Antigen) immunostaining, and confirmed that Ad-MSCs in Si-HPMC do not proliferate whatever the stiffness of the hydrogel (Fig. 1C). Since it has been established that the therapeutic benefit of MSC-based therapy is associated with their capacity to secrete a broad range of bioactive molecules, we tested the ability of Ad-MSCs embedded in 1.5% Si-HPMC (3D) to secrete growth factors involved in epithelial regeneration (IGF1-2, KGF, IL11, EGF and FGF2), pro-angiogenesis (VEGF) and anti-inflammatory processes (PGE2 and IL10), compared with Ad-MSCs cultivated in a monolayer (2D). To normalize the quantity of secreted molecules according to cell number, all the results were expressed according with DNA content. We demonstrated that Ad-MSCs mixed in the hydrogel kept

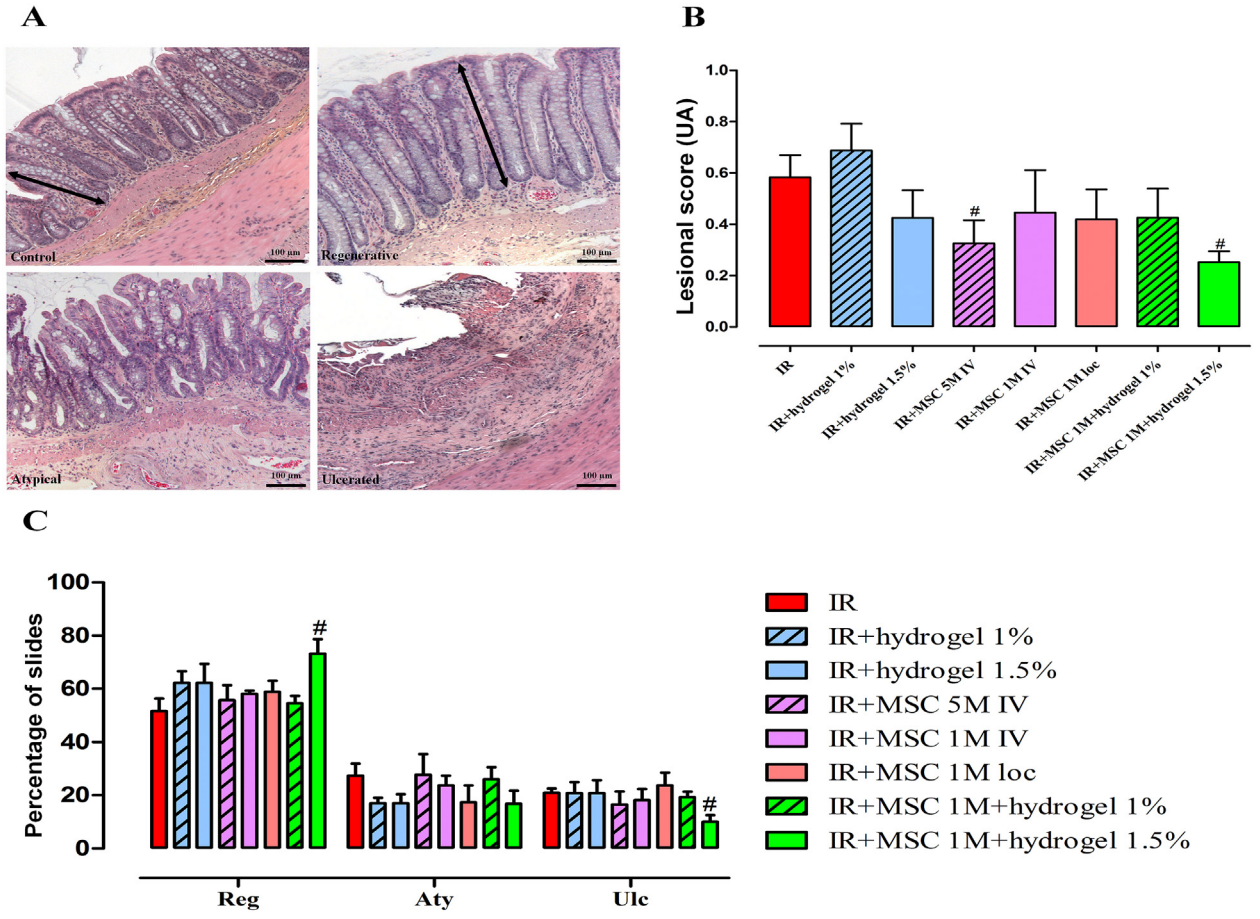

Fig. 2. Characterization of radiation-induced epithelium damage 4 weeks after irradiation. (A) Representative pictures of the lesion score used. Arrows represent colonic crypts. In a normal non-irradiated colon (top left picture), organized crypts were observed. In the regenerative zone, regenerative, elongated crypts were observed (top right picture). In the atypical zone, we distinguished atypical, disorganized crypts and small edema (bottom left picture). In the ulcerated zone, crypts were totally absent and mucosa was replaced by dense inflammatory infiltrate (bottom right picture). The sub-mucosa was characterized by an immense edema with dense extracellular matrix deposition. (B) Lesion score. (C) Percentage of slides in each area (regenerative, atypical and ulcerated area). N = 10 animals per group. IR = irradiated rats, M = million, IV = intravenous, loc = locally injected cells, Reg = regenerative, Aty = atypical, Ulc = ulcerated. $^{\#}p < 0.05$ vs. irradiated rats, $^{\#\#}p < 0.01$ vs. irradiated rats.

their ability to secrete molecules (Fig. 1D). Interestingly, Ad-MSCs embedded in 1.5% Si-HPMC were able to secrete higher concentrations of IGF-1 and PGE2 compared to Ad-MSCs in 2D.

3.3. The therapeutic benefit of Si-HPMC-assisted cell therapy on colonic epithelial structure

To determine the Ad-MSC treatment procedure that produces the greatest therapeutic benefit, we initiated *in vivo* experiments using the procedure described in section 2.8 (supplementary figure) and the histological structure of the colon was initially assessed. To analyze the improvement in the colonic structure, two quantifications were performed. In the first, we quantified the severity of the lesion (lesional score Fig. 2A and B) and in the second we measured the extent of the damage (Fig. 2C). Histological sections of normal colon showed organized crypts. In the irradiated field, three zones were differentiated according to epithelial parameters: the ulcerated, atypical and regenerative areas (Fig. 2A). The therapeutic effect of the treatments on epithelial injury was assessed in the various zones separately. In the regenerative and atypical zones, we noted that 5×10^6 of IV-injected Ad-MSCs and 1×10^6 of locally-injected Ad-MSCs in 1.5% hydrogel induced a significant reduction in the epithelial injury score one week after treatment ($p < 0.05$) (Fig. 2B).

Quantification of the number of ulcerated, atypical and regenerative slides was performed. We observed that the number of ulcerated slides was decreased ($p = 0.034$) in rats treated with 1.5% Ad-MSC + Si-HPMC compared with irradiated animals. Moreover, this latter treatment significantly increased the number of regenerative slides in comparison with irradiated animals ($p < 0.05$) (Fig. 2C). Overall, these results demonstrate that locally-injected Ad-MSCs embedded within 1.5% Si-HPMC induce a significant reduction in radiation-induced colonic epithelial damage as compared to Ad-MSCs injected intravenously or locally alone. These data also suggest that Ad-MSCs embedded in 1.5% Si-HPMC increase the regenerative process in the margins of the lesion leading to a reduction in the ulcerated area.

3.4. The therapeutic benefit of Si-HPMC-assisted cell therapy on epithelial barrier function

Intestinal permeability is one of the primordial functions of the gut epithelium and is commonly used as a marker of epithelial integrity. The colonic epithelium forms a selective barrier which prevents the penetration of luminal content (Fig. 3A). Epithelial barrier function was assessed in our experimental rat model, using the system of Ussing Chambers measuring colonic permeability to FD4 and intact HRP. Colonic irradiation induced an increase in colonic permeability to FD4 compared with control rats, (0.51673 cm/s vs. 0.926619 cm/s respectively) (Fig. 3B). Intravenous injection of Ad-MSCs did not modify colonic hyperpermeability to FD4 induced after irradiation. Locally-injected Ad-MSCs combined with 1.5% Si-HPMC significantly decreased colonic hyperpermeability to FD4 induced after irradiation (Fig. 3B). Colonic irradiation also induced a significant increase in colonic permeability to intact HRP in comparison with controls (Fig. 3C, $p < 0.05$). A significant effect on epithelial hyperpermeability to intact HRP was observed in rats treated with Ad-MSCs embedded within hydrogel at both concentrations (Fig. 3C). However, Ad-MSCs injected intravenously did not restore significantly HRP permeability to control level. It should be noted, however, that neither 1% nor 1.5% Si-HPMC injected alone had a beneficial effect on radiation-induced hyperpermeability to FD4 or HRP (Fig. 3B and C).

The colonic epithelial barrier is maintained by intercellular junctional complexes, such as Tight-Junctions (TJs) (Fig. 3A). TJs are

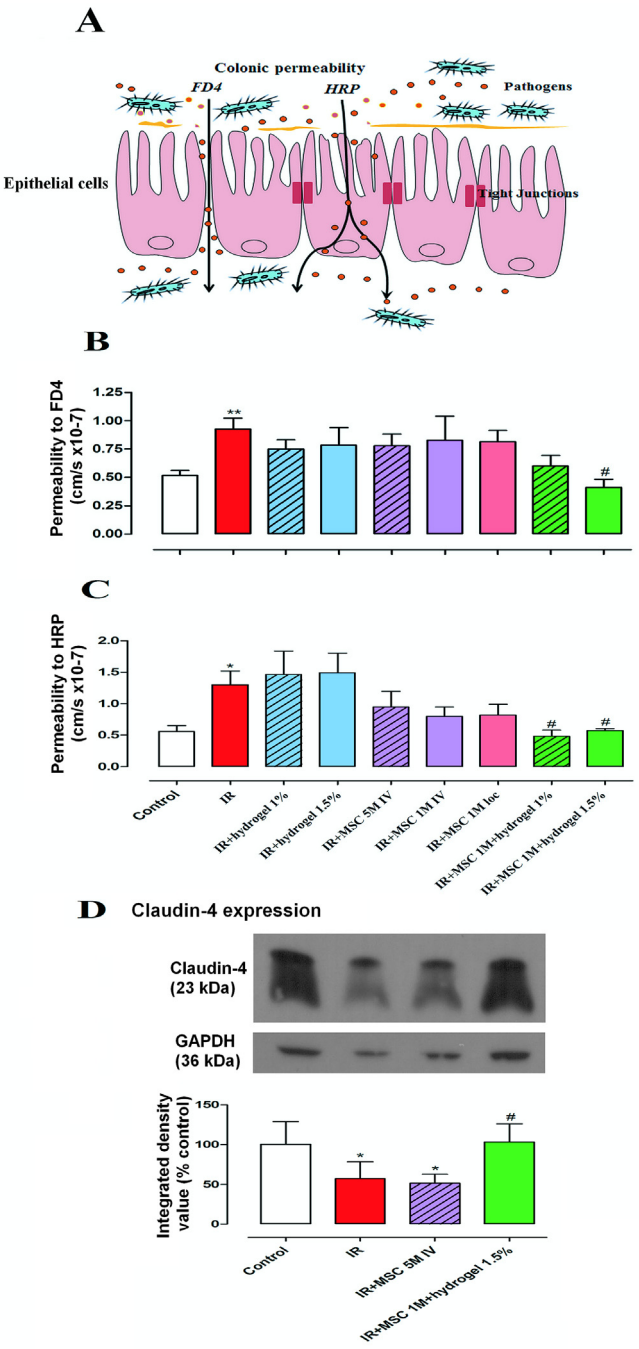

Fig. 3. Effects of biomaterial-assisted Ad-MSCs on radiation-induced changes in colonic permeability. (A) Schematic diagram of colonic epithelial barrier in physiological condition. Arrows indicate the passage of two molecules (FD4 and HRP) through epithelial cells (in pink). (B–C) Measurement of colonic permeability to FD4 and HRP using Ussing Chambers. (D) Western Blotting for claudin-4 expression. Western Blotting on colonic protein extracts was realized using claudin-4 antibody and GAPDH as internal control. Representative western blot of each group (upper) and graph representing the quantification of Claudin-4 expression after GAPDH normalization (lower). N = 16 animals per group for colonic permeability analyses and N = 6 animals per group for Western Blotting analysis. IR = irradiated rats, M = million, IV = intravenous, loc = locally injected cells. $^{*}p < 0.05$ vs. non-irradiated rats, $^{**}p < 0.01$ vs. non-irradiated rats, $^{\#}p < 0.05$ vs. irradiated rats.

composed of transmembrane proteins including claudin-4 amongst others. Western blotting experiments demonstrated a decrease in claudin-4 expression after colorectal irradiation compared with non-irradiated rats. In accordance with FD4 permeability

measurement, Ad-MSCs injected intravenously had no effect whereas local treatment with Ad-MSC+ 1.5% Si-HPMC reversed the effect of irradiation on claudin-4 expression (Fig. 3D).

3.5. Potentiation of Ad-MSC engraftment in the colonic mucosa by 1.5% Si-HPMC

To localize Ad-MSCs in the host tissue, cells were prepared from the adipose tissue of GFP-transgenic SD rats before IV or local injection into irradiated SD rats. We then analyzed Ad-MSC engraftment on colonic sections taken every 150 μm throughout the distal colon. A previous study had revealed the presence of some GFP cells in the mesentery near the vessels and in the submucosa, one week after irradiation and IV injection of MSCs [4]. Here, the number of slides with Ad-MSC GFP-positive cells was counted in each of the treated groups. In this study, Ad-MSCs were injected into established damage (3 weeks) and no GFP-positive cells could be detected in the irradiated colonic mucosa after IV treatment (data not shown). However, GFP-positive slides were observed after Ad-MSCs were injected locally with the colonoscope and greater numbers of GFP-positive slides were detected in rats treated with Ad-MSC+ 1.5% Si-HPMC (Fig. 4A and B). Moreover, when GFP-positive cells were detected on a slide, a greater amount of GFP cells was observed in the colon of rats locally injected with Ad-MSCs embedded in 1.5% Si-HPMC compared with rats locally injected with cells alone (Fig. 4B, right graph). We observed that one week after *in vivo* injection of Ad-MSCs embedded in 1.5% Si-HPMC into chronic colonic damage, most of the cells were localized at the periphery of the hydrogel and had a fibroblastic-like shape. After later time points (14 and 21 days after injection), Ad-MSC GFP-positive cells were still observed only in the group Ad-MSC + hydrogel. Lower quantity of cells was observed and they were fully protected by the hydrogel (Fig. 4C).

3.6. Fate of Ad-MSCs engrafted in irradiated colonic tissue

To analyze the behavior of locally injected Ad-MSCs in irradiated tissue, we tested their proliferative capacity and whether detected cells were apoptotic. Colorectal irradiation leads to a hostile microenvironment with high oxidative stress, ischemia and inflammation which could limit the viability of the injected cells. The proliferation of Ad-MSCs in irradiated colonic tissue was assessed using PCNA staining. One week after the injection, we observed that the majority of the cells were not proliferating independently in the presence of the hydrogel (Fig. 5A). TUNEL staining was used to detect the cells that underwent programmed cell death. In our experiments, we demonstrated that Ad-MSCs, whether embedded or not in hydrogel, are not apoptotic (Fig. 5B) (Data not shown for PCNA and TUNEL staining without hydrogel).

3.7. Si-HPMC-embedded Ad-MSC attenuates macrophage infiltrate

Macrophage infiltrate is persistent in late radiation colonic damage. Macrophages are involved in tissue clearing and initiate tissue remodeling after tissue injury, but they also play a role in perpetuating inflammation. In this study, we investigated macrophage infiltrate using CD68 antigen immunostaining (Fig. 6). We demonstrated that one week after injection of 1.5% Si-HPMC alone in the irradiated mucosa, few CD68-positive cells were detected. A greater amount of macrophages was detected near Ad-MSC-implanted cells compared with Ad-MSCs embedded in Si-HPMC (Fig. 6A and B).

To understand the mechanism of action by which Ad-MSCs + Si-HPMC could decrease macrophage infiltrate, we questioned whether the secretion of chemoattractant molecules by Ad-MSCs is

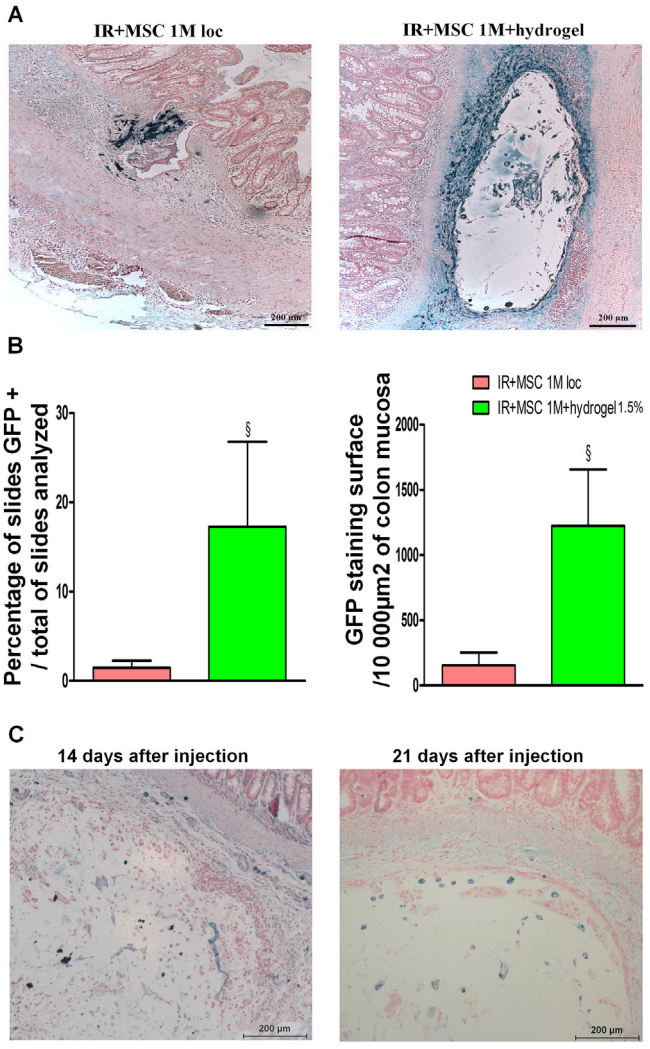

Fig. 4. Ad-MSC engraftment in colonic sub-mucosa after injection. (A) Representative pictures of GFP-Ad-MSCs after IHC (in blue) in the irradiated colonic sub-mucosa 7 days after local injection of GFP-Ad-MSCs (left) or GFP-Ad-MSCs embedded in 1.5% hydrogel (right). (B) Quantification of the GFP-Ad-MSCs engraftment. The extent of GFP-Ad-MSCs engraftment in the irradiated colon is quantified by the percentage of slides GFP-Ad-MSC-positive cells among the total of analyzed slides (left). The quantity of GFP-Ad-MSCs engrafted cells was also quantified using histolab software. On the GFP positive slides, the surface of GFP staining is evaluated among 10 000 μm^2 of tissue surface (right). (C) Later time point engraftment analyses of locally injected Ad-MSCs in 1.5% hydrogel. Representative pictures of GFP-Ad-MSCs after IHC (in blue) in the irradiated colonic sub-mucosa 14 days (left) and 21 days. N = 8 animals per group. IR = irradiated rats, M = million, loc = locally injected cells. $^{\S}p < 0.05$ vs. irradiated rats locally injected with Ad-MSCs without hydrogel.

modified by their embedding in 1.5% Si-HPMC. Moreover, chronic side effects induced after irradiation are associated with IL1b and TGFb cytokine secretion. Therefore, we also tested the secretion capacities of Ad-MSCs after these pro-inflammatory stimulations retracing the *in vivo* situation. Using an ELISA assay, we demonstrated that in the absence of stimulation, embedding cells in hydrogel did not modify the chemoattractant secretion profiles (Fig. 7A). However, when Ad-MSCs were stimulated with IL-1b and TGF-b, as in an *in vivo* situation, it was shown that Ad-MSCs secreted fewer chemoattractant molecules in 3D than in 2D (Fig. 7A). Numerous studies demonstrated that Ad-MSCs secrete anti-inflammatory molecules as well as high quantity of VEGF molecule involved in pro-angiogenesis process. In this study, we analyzed the modifications of these molecules following hydrogel-

embedding and stimulations (Fig. 7B). We determined that PGE2 secretion is increased in 3D conditions, however IL10 is not modified after hydrogel embedding and Il1b + TGFb stimulations. We also demonstrated that stimulated Ad-MSCs secrete more VEGF in 3D compared with 2D configuration (Fig. 7B).

4. Discussion

Intravenous injection of MSCs has been shown to improve the intestinal regeneration process after irradiation [3,4,9,29]. The reparative potential of MSCs has been shown to be mediated by the release of a broad spectrum of soluble factors [8]. Systemic infusion of MSCs has been promulgated as a simple, reproducible and safe delivery strategy for use in clinics [7,18]. The ability of MSCs to host injured tissues may result in localized therapeutic benefits. However, the potential of MSC migration to the injured organs after intravenous (IV) injection is impeded by cell trapping within the lung [14]. Moreover, the optimal time-point for IV MSC delivery is unknown and is dependent upon the secretion of chemoattractant molecules like SDF1α [30]. In view of the uncertain fate of IV-injected cells, local injection of MSCs, implanted directly into the lesion site, which has been tested in different tissues [31,32], allows fewer cells to be injected and provides a greater therapeutic benefit [31]. For the first time, this study proposes and demonstrates the feasibility of colonoscopy to deliver MSCs directly into the colon without surgery, using imaging and syringe catheter systems. However, once injected into the injured tissue the cell survival rate could be limited due to the ischemic and inflammatory microenvironment induced after irradiation. Growing evidence suggests that synthetic biomaterials are an encouraging approach to sustaining the long-term cell viability of stem cells *in situ*, by creating an optimal niche that preserves the cells. These scaffolds offer the potential to appropriately deliver cells into the injured site, optimizing the therapeutic effect of stem cell therapy. Amongst the biomaterials used in regenerative medicine, hydrogels are likely the most suitable materials since they display injectability and cross-linking properties. We used a Si-HPMC hydrogel that displays rheological properties appropriate to its implantation via mini-invasive surgery [26]. The advantage of this hydrogel is its self-setting property without any addition of cross-linking toxic agents. It is a hydrophilic and neutral hydrogel with no bioactivity. Its influence is to provide a protective barrier and to maintain the cell in a non-adherent shape. It has already been demonstrated that intra-myocardial delivery of MSC-embedded Si-HPMC preserves cardiac function after myocardial infarction [22]. Intra-colonic injection of Ad-MSCs has not yet been proposed as a pre-clinical treatment for radiation-induced colorectal damage. In this study, we established Si-HPMC with rheological properties that can be loaded through the syringe catheter system of a colonoscope. The gelation time of Si-HPMC has been determined to enable a cell-hydrogel mixture as well as its injection *in vivo*. This time is suitable for manipulation in an operating theatre and could be used by surgeons. Furthermore, we demonstrated that Ad-MSCs in Si-HPMC are 95% viable for up to 21 days *in vitro* and are biologically active. Indeed, we determined that Ad-MSCs in 3D configuration in 1.5% Si-HPMC displayed a round shape *in vitro* that has no influence on their ability to secrete molecules involved in epithelial regeneration, angiogenesis or the anti-inflammatory process.

MSCs from bone marrow have been used to treat radiation-induced proctitis in patients over-irradiated at Epinal hospital. It has been demonstrated that MSCs reduced pain and the number of episodes of diarrhea in three patients who were resistant to symptomatic treatments [6]. The aim of this study was to find a novel clinically-applicable procedure for MSC treatment of colorectal damage that improves the therapeutic benefit whilst at the same time decreasing the number of injected cells. We used a rat model of gastrointestinal complications following radiotherapy. Patients treated for rectal adenocarcinoma with preoperative radiotherapy receive a total dose of 45Gy, delivered in fraction of 1.8 or 2Gy. However, previous works performed in rats showed no changes on colonic structure after fractionated irradiation [33]. Here, the irradiation methodology used is a single dose of 29 Gy which induces severe colorectal damage similar to that observed in patients subjected to radiotherapy [4]. We analyzed the structure and intestinal permeability which is one of the primordial functions of the gut epithelium and is commonly used as a marker of epithelial integrity. Increased intestinal permeability has already been demonstrated in rat ileum after 5Gy abdominal irradiation [34,35]. This result has been confirmed in patients affected by breast cancer, sarcoma and colorectal cancer treated with different chemotherapy agents or after radiotherapy [36–40]. In our rat model of severe and chronic radiation-induced damage [3], we demonstrated an alteration of the colonic histological structure associated with an increase in epithelial permeability of colon/rectum segments to FD4 and HRP macromolecules 4 weeks after irradiation. These data are of particular importance, and demonstrate the clinical relevance of our animal model, since the colon delivers a plentiful source of luminal antigens within the range of molecular weights herein assessed, which may generate mucosal injury and be a reservoir of systemic infections [41].

This study confirmed previous results demonstrating the therapeutic benefit of 5 million IV-injected Ad-MSCs on epithelial structure after localized irradiation [5]. A decrease in the number of cells (1 million), whether IV- or locally-injected, has no therapeutic

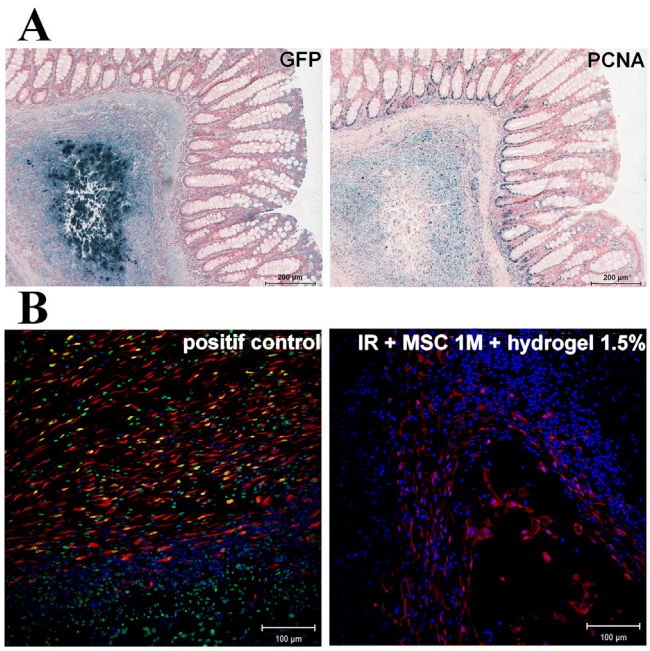

Fig. 5. Fate of Ad-MSC+1.5% Si-HPMC engrafted in irradiated colonic tissue 7 days after injection. (A) Analyses of Ad-MSC proliferation. Representative pictures of serial slides of GFP immunostaining (in blue, left picture) and PCNA immunostaining (in blue, right picture). GFP-positive cells were localized in the center whereas PCNA immunostaining at the periphery determining that few Ad-MSCs were proliferating in vivo when they were injected in the hydrogel. (B) Analyses of Ad-MSC apoptosis using TUNEL assay. Ad-MSCs are stained in red and apoptotic cells are stained in green. Cells stained in yellow (dual stained red and green) upon analysis represent apoptotic cells. Representative pictures of the positive control (cell death is induced by DNase treatment) and irradiated rats injected with 1 million Ad-MSCs locally with the hydrogel (1.5%). No yellow cells were detected determining that Ad-MSCs were not apoptotic in the hydrogel. N = 8 animals per group. IR = irradiated rats, M = million.

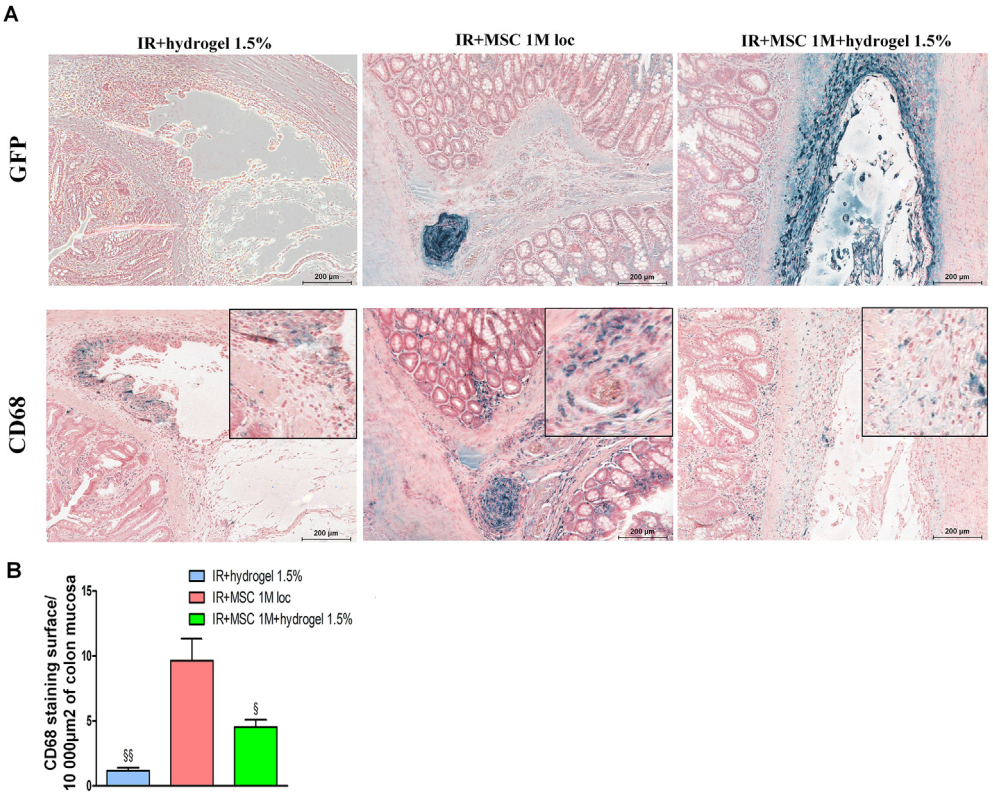

Fig. 6. Macrophage infiltrate near implanted Ad-MSCs. (A) Representative pictures of serial slides of GFP immunostaining (in blue, top pictures) and CD68 immunostaining (in blue, bottom pictures) 7 days after injection. Squares in the bottom pictures represent an enlargement of the areas after CD68 immunostaining. CD68 imunostaining is more important when Ad-MSCs were injected alone (bottom middle picture) in comparison with Ad-MSCs embedded in Si-HPMC (bottom right picture). (B) Quantification of CD68 infiltrate, the surface of CD68 staining is evaluated among 10 000µ2 of tissue surface. N = 8 animals per group. IR = irradiated rats, M = million, loc = locally injected cells. $^{\S}p < 0.05$ vs. irradiated rats locally injected with Ad-MSCs without hydrogel, $^{\S\S}p < 0.01$ vs. irradiated rats locally injected with Ad-MSCs without hydrogel.

effect. We also observed that Ad-MSCs embedded in 1% Si-HPMC produced no improvement in epithelial structure. This result can be explained by our *in-vitro* observations demonstrating that the rheological properties of 1% Si-HPMC do not allow entrapment of all the cells since some cells remain attached to the culture dish and are not inside the hydrogel. However, Ad-MSCs embedded in 1.5% Si-HPMC statistically improved all the parameters tested in this study. This therapeutic benefit is associated with an increase in Ad-MSC engraftment in the colonic mucosa compared to all other groups. Different therapeutic effects have been proposed for MSCs, but it is now well established that the paracrine effect is the most prevalent rather than differentiation or transdifferentiation in epithelial cells [42,43]. They have been shown to act therapeutically by releasing pro-regenerative factors and/or by modulating the immune response through several factors [44]. Thus, increasing Ad-MSC engraftment could help improve their therapeutic benefit. Moreover, we determined that 7 days after *in vivo* injection in the irradiated colonic mucosa, Ad-MSCs embedded in 1.5% hydrogel were not apoptotic. It could be hypothesized that 1.5% Si-HPMC preserves the cells at various levels. It has been reported that the cells are protected from mechanical forces, by the hydrogel, during syringe needle flow [45]. This result suggests that cells could be protected by Si-HPMC in the early stages of the treatment process. Moreover, when Ad-MSCs were recovered after culture expansion, then injected in saline solution into the tissue, their lack of adhesion to extracellular matrix can promote apoptotic signaling. 1.5% Si-HPMC could therefore be an appropriate scaffold to maintain cell viability within the tissue and derive a therapeutic benefit. Indeed, strategies using genetically-modified MSCs to decrease their apoptosis have been successfully applied in animal models [46,47]. These interesting experiments shed light on the correlation between the therapeutic benefit and the inhibition of MSC apoptosis. However, their use in clinics cannot be applied at present. Another hypothesis is that 1.5% Si-HPMC could protect the cells from the inflammatory environment induced after irradiation. It has been demonstrated that irradiation induces chronic secretion of pro-inflammatory molecules as IL1b and TGFb [19,48] and reactive oxygen species [49]. However, it has been observed that molecules are able to diffuse through the scaffold. Therefore under these conditions, we observed a statistical increase in VEGF secretion in 3D after stimulation with IL1b and TGFb. It is therefore likely that Ad-MSCs in 1.5% Si-HPMC are able to resist the inflammatory environment. Indeed, MSCs have been shown to resist irradiation due to their high antioxidant capacities [50]. Moreover, it is now acknowledged that the inflammatory environment to which MSCs are exposed plays a pivotal role in activating their immunosuppressive functions [51]. As macrophage infiltrate is persistent in late radiation colonic damage [19,20], our analyses focused on this type of innate immune cells. We observed that high infiltration of macrophages was seen in the vicinity of Ad-MSCs that were not embedded within the hydrogel. Interestingly, there were fewer $CD68^{+}$ macrophages near Ad-MSCs embedded in 1.5% Si-HPMC. This observation led us to hypothesize that Ad-MSCs were recognized by host macrophages in a non-consanguinous situation. This fact has also been observed in another study [52] and various hypotheses could be made. It has been argued that the culture expansion modified membrane protein expression of MSCs, particularly with modification of HLA membrane expression,

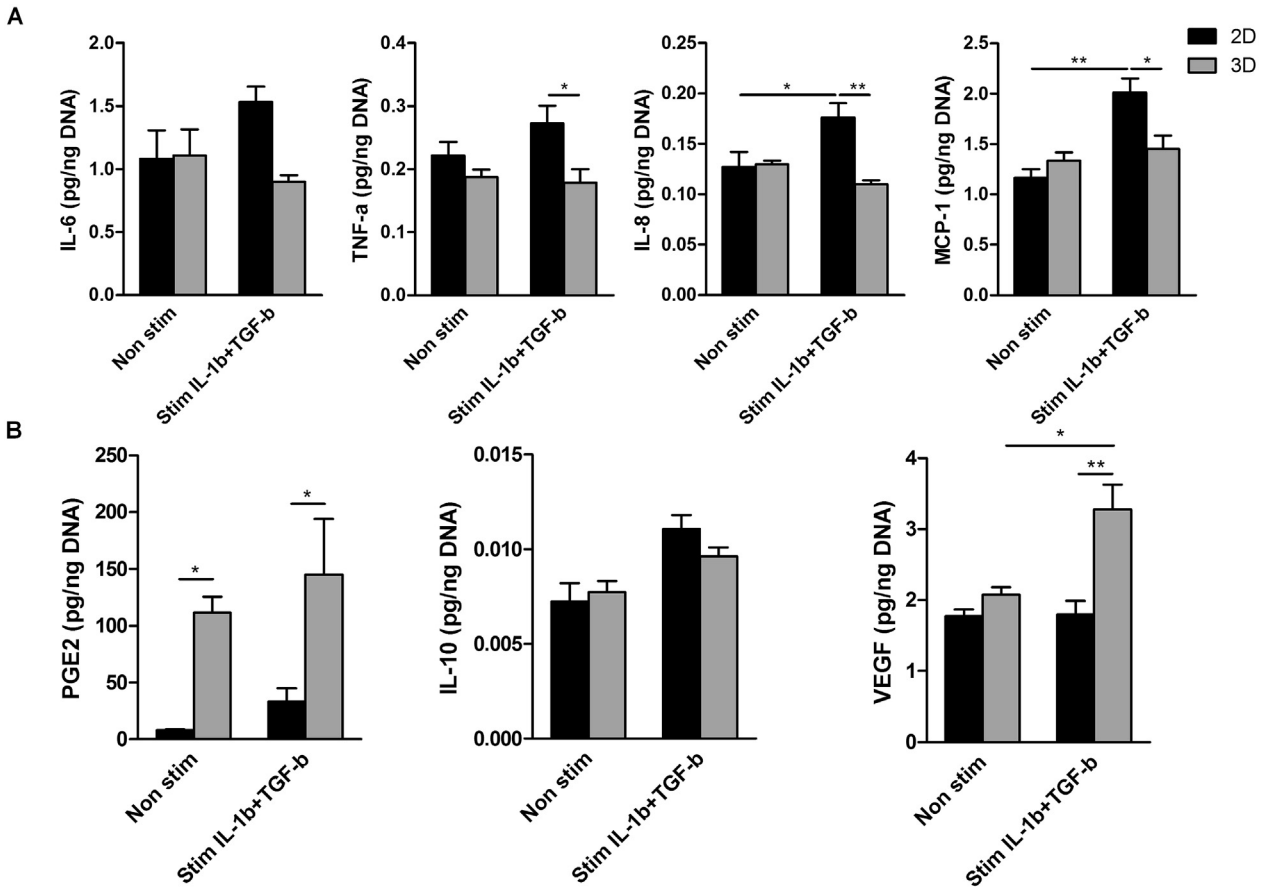

Fig. 7. Secretion factors of Ad-MSCs in Si-HPMC compared with two-dimensional Ad-MSCs. (A) Graphs represent the chemokine contents of the supernatant of Ad-MSCs stimulated or not with IL1b and TGFb. Ad-MSCs stimulated with IL1b and TGFb secreted less chemoattractants compared with Ad-MSCs embedded in 1.5% Si-HPMC. (B) Graphs represent PGE2 and IL10 (anti-inflammatory) and VEGF (pro-angiogenic) contents of the supernatant of Ad-MSCs stimulated or not with IL1b and TGFb. All the results were normalized by DNA quantification. N = 3 donors in triplicate. $^{*}p < 0.05$, $^{**}p < 0.01$.

potentially inducing recognition by macrophages [53,54]. Another explanation is the initialization of tissue clearing by macrophages in the presence of a huge amount of exogenous cells in the tissue structure. Indeed, it has been demonstrated that autologous MSCs injected in immune-deficient mice lacking T, B and NK cells have a short survival time [15], indicating that other cell types, like macrophages, could contribute to the clearance of MSCs. Interestingly, our results demonstrated limited macrophage infiltrate near the hydrogel-embedded Ad-MSCs. This result is of particular importance since 1.5% Si-HPMC seems to protect Ad-MSCs from the macrophages. In the context of a clinical application, it will be interesting to test whether the same result is observed with Ad-MSCs from other strains embedded in Si-HPMC.

To understand the molecular mechanism of macrophage infiltration modulation, we analyzed the secretion of chemoattractant molecules by Ad-MSCs, in a native context or stimulated by IL1b and TGFb which are secreted in colonic mucosa after irradiation. We observed that the secretion of IL-8 and MCP-1 in particular, is higher in non-entrapped cells than in Ad-MSCs in 3D after stimulation with IL1b and TGFb. These results suggest a modification of the phenotype of Si-HPMC-embedded MSC compared to cells in culture plastic flask. Various studies already demonstrated a modification of secretion abilities when the cells are in 3D compared with cells cultured in monolayer [21,55,56]. Moreover, it has also been suggested that 3D culture conditions are closest of the *in vivo* environment compared with the simplicity of 2D culture that seems a reductionist approaches to understand the physiological behavior of cells [57]. Besides, a recent study demonstrated that topographical cues influence the soluble factors secreted by MSCs and modify the communication between MSCs and macrophages [56]. Similarly, Swartzlander et al. have demonstrated that MSCs embedded in synthetic hydrogel were able to attenuate macrophage activation [58]. These findings are of great importance and suggest that MSCs may be able to combat foreign body response (FBR) via macrophage cross-talk, the primary orchestrators of FBR [59]. Altogether, these data could explain our *in vivo* observations, highlighting a decrease in $CD68^{+}$ macrophages near the hydrogel embedded with Ad-MSCs compared with Ad-MSCs alone. Our results suggest that the hydrogel exerts an immunoprotective function through two mechanisms: a decrease in macrophage chemoattractant secretion by embedded cells in a pro-inflammatory context and a delay in the tissue clearance of Ad-MSCs trapped in the hydrogel.

In conclusion, we developed a Si-HPMC with rheological properties compatible with injection through a colonoscope catheter. The defined properties are compatible with use by surgeons in an operating theatre. We demonstrated that Ad-MSCs embedded in 1.5% Si-HPMC are biologically active in normal conditions and are also able to modulate their secretome according to the inflammatory context. Using a clinically-relevant animal model, we determined that local injection of 1 million Ad-MSCs embedded in 1.5% Si-HPMC hydrogel improves the structure of colonic mucosa damaged after irradiation. Ad-MSCs injected according to this protocol have a greater therapeutic benefit on colonic function

measured by epithelial permeability compared with the intravenous injection of Ad-MSCs which is the protocol currently used in clinics. This therapeutic benefit is associated with increased engraftment of viable Ad-MSCs in the colonic submucosa. This study also shows, for the first time, that Ad-MSCs embedded in 1.5% Si-HPMC are able to reduce macrophage infiltration *in vivo* near the injection point. This innovative procedure produces encouraging results and may represent a breakthrough in the use of stem cell-assisted biomaterial therapy. This approach will allow a mini-invasive intervention and could be proposed to patients suffering from late radiotherapy side effects.

Author contributions

LM: conception and design, data collection, data analyses and interpretation, statistical analysis and manuscript writing. GP, BD, S-L B and CD: data collection and interpretation. AS: data interpretation. MB and RT: data interpretation and manuscript correction. JG, PW, GR: conception and design, financial support, data interpretation and manuscript correction. NM: conception and design, financial support, data interpretation and manuscript writing. All authors read and approved the final manuscript.

Conflict of interest

The authors have no conflict of interest to declare.

Acknowledgments

We thank Yoann Ristic and the GSEA team for their assistance with animals. This work was supported by the Agence Nationale de la Recherche (ANR-13-RPIB-0008). LM and GP were supported by the ANR 13-RPIB-0008 “ANTHOS”.

Appendix A. Supplementary data

Supplementary data related to this article can be found at http://dx.doi.org/10.1016/j.biomaterials.2016.11.017.

References

[1] L. Moussa, B. Usunier, C. Demarquay, M. Benderitter, R. Tamarat, A. Semont, et al., Bowel Radiation Injury: complexity of the pathophysiology and promises of cell and tissue engineering, Cell Transplant. (2016) [Epub ahead of print].
[2] B. Usunier, M. Benderitter, R. Tamarat, A. Chapel, Management of fibrosis: the mesenchymal stromal cells breakthrough, Stem Cells Int. 2014 (2014) 340257.
[3] A. Semont, M. Mouiseddine, A. Francois, C. Demarquay, N. Mathieu, A. Chapel, et al., Mesenchymal stem cells improve small intestinal integrity through regulation of endogenous epithelial cell homeostasis, Cell Death Differ. 17 (2010) 952–961.
[4] A. Semont, C. Demarquay, R. Bessout, C. Durand, M. Benderitter, N. Mathieu, Mesenchymal stem cell therapy stimulates endogenous host progenitor cells to improve colonic epithelial regeneration, PloS One 8 (2013) e70170.
[5] R. Bessout, C. Demarquay, L. Moussa, A. Rene, B. Doix, M. Benderitter, et al., TH17 predominant T-cell responses in radiation-induced bowel disease are modulated by treatment with adipose-derived mesenchymal stromal cells, J. Pathol. 237 (2015) 435–446.
[6] D. Peiffert, J.M. Simon, F. Eschwege, [Epinal radiotherapy accident: passed, present, future], Cancer Radiother. J. de la Soc. Francaise de Radiother. Oncol. 11 (2007) 309–312.
[7] J. Voswinkel, S. Francois, J.M. Simon, M. Benderitter, N.C. Gorin, M. Mohty, et al., Use of mesenchymal stem cells (MSC) in chronic inflammatory fistulizing and fibrotic diseases: a comprehensive review, Clin. Rev. Allergy Immunol. 45 (2013) 180–192.
[8] A.I. Caplan, J.E. Dennis, Mesenchymal stem cells as trophic mediators, J. Cell. Biochem. 98 (2006) 1076–1084.
[9] C. Linard, E. Busson, V. Holler, C. Strup-Perrot, J.V. Lacave-Lapalun, B. Lhomme, et al., Repeated autologous bone marrow-derived mesenchymal stem cell injections improve radiation-induced proctitis in pigs, Stem Cells Transl. Med. 2 (2013) 916–927.
[10] U.M. Fischer, M.T. Harting, F. Jimenez, W.O. Monzon-Posadas, H. Xue, S.I. Savitz, et al., Pulmonary passage is a major obstacle for intravenous stem cell delivery: the pulmonary first-pass effect, Stem Cells Dev. 18 (2009) 683–692.
[11] R.H. Lee, A.A. Pulin, M.J. Seo, D.J. Kota, J. Ylostalo, B.L. Larson, et al., Intravenous hMSCs improve myocardial infarction in mice because cells embolized in lung are activated to secrete the anti-inflammatory protein TSG-6, Cell Stem Cell 5 (2009) 54–63.
[12] J.W. Jung, M. Kwon, J.C. Choi, J.W. Shin, I.W. Park, B.W. Choi, et al., Familial occurrence of pulmonary embolism after intravenous, adipose tissue-derived stem cell therapy, Yonsei Med. J. 54 (2013) 1293–1296.
[13] D. Furlani, M. Ugurlucan, L. Ong, K. Bieback, E. Pittermann, I. Westien, et al., Is the intravascular administration of mesenchymal stem cells safe? Mesenchymal stem cells and intravital microscopy, Microvasc. Res. 77 (2009) 370–376.
[14] M.J. Hoogduijn, M. Roemeling-van Rhijn, A.U. Engela, S.S. Korevaar, F.K. Mensah, M. Franquesa, et al., Mesenchymal stem cells induce an inflammatory response after intravenous infusion, Stem Cells Dev. 22 (2013) 2825–2835.
[15] E. Eggenhofer, V. Benseler, A. Kroemer, F.C. Popp, E.K. Geissler, H.J. Schlitt, et al., Mesenchymal stem cells are short-lived and do not migrate beyond the lungs after intravenous infusion, Front. Immunol. 3 (2012) 297.
[16] T.G. Ebrahimian, F. Pouzoulet, C. Squiban, V. Buard, M. Andre, B. Cousin, et al., Cell therapy based on adipose tissue-derived stromal cells promotes physiological and pathological wound healing, Arterioscler. Thromb. Vasc. Biol. 29 (2009) 503–510.
[17] E. Bey, M. Prat, P. Duhamel, M. Benderitter, M. Brachet, F. Trompier, et al., Emerging therapy for improving wound repair of severe radiation burns using local bone marrow-derived stem cell administrations, Wound Repair Regen. Off. Publ. Wound Heal. Soc. Eur. Tissue Repair Soc. 18 (2010) 50–58.
[18] M.M. Lalu, L. McIntyre, C. Pugliese, D. Fergusson, B.W. Winston, J.C. Marshall, et al., Safety of cell therapy with mesenchymal stromal cells (SafeCell): a systematic review and meta-analysis of clinical trials, PloS One 7 (2012) e47559.
[19] R. Bessout, A. Semont, C. Demarquay, A. Charcosset, M. Benderitter, N. Mathieu, Mesenchymal stem cell therapy induces glucocorticoid synthesis in colonic mucosa and suppresses radiation-activated T cells: new insights into MSC immunomodulation, Mucosal Immunol. 7 (2014) 656–669.
[20] K. Blirando, F. Milliat, I. Martelly, J.C. Sabourin, M. Benderitter, A. Francois, Mast cells are an essential component of human radiation proctitis and contribute to experimental colorectal damage in mice, Am. J. Pathol. 178 (2011) 640–651.
[21] N. Landazuri, R.D. Levit, G. Joseph, J.M. Ortega-Legaspi, C.A. Flores, D. Weiss, et al., Alginate microencapsulation of human mesenchymal stem cells as a strategy to enhance paracrine-mediated vascular recovery after hindlimb ischaemia, J. Tissue Eng. Regen. Med. 10 (2016) 222–232.
[22] E. Mathieu, G. Lamirault, C. Toquet, P. Lhommet, E. Rederstorff, S. Sourice, et al., Intramyocardial delivery of mesenchymal stem cell-seeded hydrogel preserves cardiac function and attenuates ventricular remodeling after myocardial infarction, PloS One 7 (2012) e51991.
[23] C. Vinatier, C. Bouffi, C. Merceron, J. Gordeladze, J.M. Brondello, C. Jorgensen, et al., Cartilage tissue engineering: towards a biomaterial-assisted mesenchymal stem cell therapy, Curr. Stem Cell Res. Ther. 4 (2009) 318–329.
[24] X. Bourges, P. Weiss, G. Daculsi, G. Legeay, Synthesis and general properties of silated-hydroxypropyl methylcellulose in prospect of biomedical use, Adv. Colloid Interface Sci. 99 (2002) 215–228.
[25] S. Allahbash, T. Nicolai, C. Chassenieux, J.F. Tassin, L. Benyahia, P. Weiss, et al., Interplay of thermal and covalent gelation of silanized hydroxypropyl methyl cellulose gels, Carbohydr. Polym. 115 (2015) 510–515.
[26] A. Fatimi, J.F. Tassin, S. Quillard, M.A. Axelos, P. Weiss, The rheological properties of silated hydroxypropylmethylcellulose tissue engineering matrices, Biomaterials 29 (2008) 533–543.
[27] A.C. Maehly, B. Chance, The assay of catalases and peroxidases, Methods Biochem. Anal. 1 (1954) 357–424.
[28] P. Artursson, C. Magnusson, Epithelial transport of drugs in cell culture. II: effect of extracellular calcium concentration on the paracellular transport of drugs of different lipophilicities across monolayers of intestinal epithelial (Caco-2) cells, J. Pharm. Sci. 79 (1990) 595–600.
[29] P. Chang, Y. Qu, Y. Liu, S. Cui, D. Zhu, H. Wang, et al., Multi-therapeutic effects of human adipose-derived mesenchymal stem cells on radiation-induced intestinal injury, Cell Death Dis. 4 (2013) e685.
[30] J. Zhang, J.F. Gong, W. Zhang, W.M. Zhu, J.S. Li, Effects of transplanted bone marrow mesenchymal stem cells on the irradiated intestine of mice, J. Biomed. Sci. 15 (2008) 585–594.
[31] T. Freyman, G. Polin, H. Osman, J. Crary, M. Lu, L. Cheng, et al., A quantitative, randomized study evaluating three methods of mesenchymal stem cell delivery following myocardial infarction, Eur. Heart J. 27 (2006) 1114–1122.
[32] J.J. Lataillade, C. Doucet, E. Bey, H. Carsin, C. Huet, I. Clairand, et al., New approach to radiation burn treatment by dosimetry-guided surgery combined with autologous mesenchymal stem cell therapy, Regen. Med. 2 (2007) 785–794.
[33] O. Gremy, M. Benderitter, C. Linard, Acute and persisting Th2-like immune response after fractionated colorectal gamma-irradiation, World J. Gastroenterol. 14 (2008) 7075–7085.
[34] M. Porvaznik, Tight junction disruption and recovery after sublethal gamma irradiation, Radiat. Res. 78 (1979) 233–250.
[35] Z. Somosy, J. Kovacs, L. Siklos, G.J. Koteles, Morphological and histochemical

changes in intercellular junctional complexes in epithelial cells of mouse small intestine upon X-irradiation: changes of ruthenium red permeability and calcium content, Scanning Microsc. 7 (1993) 961–971.
[36] B. Daniele, M. Secondulfo, R. De Vivo, S. Pignata, L. De Magistris, P. Delrio, et al., Effect of chemotherapy with 5-fluorouracil on intestinal permeability and absorption in patients with advanced colorectal cancer, J. Clin. Gastroenterol. 32 (2001) 228–230.
[37] B. Fazeny-Dorner, M. Veitl, C. Wenzel, T. Brodowicz, C. Zielinski, M. Muhm, et al., Alterations in intestinal permeability following the intensified polydrug-chemotherapy IFADIC (ifosfamide, Adriamycin, dacarbazine), Cancer Chemother. Pharmacol. 49 (2002) 294–298.
[38] G. Parrilli, R.V. Iaffaioli, M. Martorano, R. Cuomo, S. Tafuto, M.G. Zampino, et al., Effects of anthracycline therapy on intestinal absorption in patients with advanced breast cancer, Cancer Res. 49 (1989) 3689–3691.
[39] P. Nejdfors, M. Ekelund, B.R. Westrom, R. Willen, B. Jeppsson, Intestinal permeability in humans is increased after radiation therapy, Dis. Colon Rectum 43 (2000) 1582–1587 discussion 7–8.
[40] J. Dvorak, B. Melichar, R. Hyspler, L. Krcmova, L. Urbanek, H. Kalabova, et al., Intestinal permeability, vitamin A absorption, alpha-tocopherol, and neopterin in patients with rectal carcinoma treated with chemoradiation, Med. Oncol. 27 (2010) 690–696.
[41] J.R. Turner, Intestinal mucosal barrier function in health and disease, Nat. Rev. Immunol. 9 (2009) 799–809.
[42] A.I. Caplan, D. Correa, The MSC: an injury drugstore, Cell Stem Cell 9 (2011) 11–15.
[43] X. Liang, Y. Ding, Y. Zhang, H.F. Tse, Q. Lian, Paracrine mechanisms of mesenchymal stem cell-based therapy: current status and perspectives, Cell Transplant. 23 (2014) 1045–1059.
[44] J.D. Glenn, K.A. Whartenby, Mesenchymal stem cells: emerging mechanisms of immunomodulation and therapy, World J. Stem Cells 6 (2014) 526–539.
[45] B.A. Aguado, W. Mulyasasmita, J. Su, K.J. Lampe, S.C. Heilshorn, Improving viability of stem cells during syringe needle flow through the design of hydrogel cell carriers, Tissue Eng. Part A 18 (2012) 806–815.
[46] A.A. Mangi, N. Noiseux, D. Kong, H. He, M. Rezvani, J.S. Ingwall, et al., Mesenchymal stem cells modified with Akt prevent remodeling and restore performance of infarcted hearts, Nat. Med. 9 (2003) 1195–1201.
[47] X. Xue, Y. Liu, J. Zhang, T. Liu, Z. Yang, H. Wang, Bcl-xL genetic modification enhanced the therapeutic efficacy of mesenchymal stem cell transplantation in the treatment of heart infarction, Stem Cells Int. 2015 (2015) 176409.
[48] M. Boerma, J. Wang, K.K. Richter, M. Hauer-Jensen, Orazipone, a locally acting immunomodulator, ameliorates intestinal radiation injury: a preclinical study in a novel rat model, Int. J. Radiat. Oncol. Biol. Phys. 66 (2006) 552–559.
[49] C. Haton, A. Francois, M. Vandamme, J. Wysocki, N.M. Griffiths, M. Benderitter, Imbalance of the antioxidant network of mouse small intestinal mucosa after radiation exposure, Radiat. Res. 167 (2007) 445–453.
[50] M.F. Chen, C.T. Lin, W.C. Chen, C.T. Yang, C.C. Chen, S.K. Liao, et al., The sensitivity of human mesenchymal stem cells to ionizing radiation, Int. J. Radiat. Oncol. Biol. Phys. 66 (2006) 244–253.
[51] M. Krampera, L. Cosmi, R. Angeli, A. Pasini, F. Liotta, A. Andreini, et al., Role for interferon-gamma in the immunomodulatory activity of human bone marrow mesenchymal stem cells, Stem Cells 24 (2006) 386–398.
[52] A. Tassoni, A. Gutteridge, A.C. Barber, A. Osborne, K.R. Martin, Molecular mechanisms mediating retinal reactive gliosis following bone marrow mesenchymal stem cell transplantation, Stem Cells 33 (2015) 3006–3016.
[53] P.A. Dighe, P. Viswanathan, A.K. Mruthunjaya, R.N. Seetharam, Effect of bFGF on HLA-DR expression of human bone marrow-derived mesenchymal stem cells, J. Stem Cells 8 (2013) 43–57.
[54] P.A. Sotiropoulou, S.A. Perez, M. Salagianni, C.N. Baxevanis, M. Papamichail, Characterization of the optimal culture conditions for clinical scale production of human mesenchymal stem cells, Stem Cells 24 (2006) 462–471.
[55] B. Follin, M. Juhl, S. Cohen, A.E. Pedersen, M. Gad, J. Kastrup, et al., Human adipose-derived stromal cells in a clinically applicable injectable alginate hydrogel: phenotypic and immunomodulatory evaluation, Cytotherapy 17 (2015) 1104–1118.
[56] G. Valles, F. Bensiamar, L. Crespo, M. Arruebo, N. Vilaboa, L. Saldana, Topographical cues regulate the crosstalk between MSCs and macrophages, Biomaterials 37 (2015) 124–133.
[57] B.M. Baker, C.S. Chen, Deconstructing the third dimension: how 3D culture microenvironments alter cellular cues, J. Cell Sci. 125 (2012) 3015–3024.
[58] M.D. Swartzlander, A.K. Blakney, L.D. Amer, K.D. Hankenson, T.R. Kyriakides, S.J. Bryant, Immunomodulation by mesenchymal stem cells combats the foreign body response to cell-laden synthetic hydrogels, Biomaterials 41 (2015) 79–88.
[59] J.M. Anderson, A. Rodriguez, D.T. Chang, Foreign body reaction to biomaterials, Semin. Immunol. 20 (2008) 86–100.